

# Synthesis, Crystal Structure, and Electrochemical Properties of a Simple Magnesium Electrolyte for Magnesium/Sulfur Batteries

Wanfei Li, Shuang Cheng, Jian Wang, Yongcai Qiu, Zhaozhao Zheng, Hongzhen Lin, Sanjay Nanda, Qian Ma, Yan Xu, Fangmin Ye, Meinan Liu, Lisha Zhou, and Yuegang Zhang\*

**Abstract:** Most simple magnesium salts tend to passivate the Mg metal surface too quickly to function as electrolytes for Mg batteries. In the present work, an electroactive salt  $[\text{Mg}(\text{THF})_6][\text{AlCl}_4]_2$  was synthesized and structurally characterized. The Mg electrolyte based on this simple mononuclear salt showed a high Mg cycling efficiency, good anodic stability (2.5 V vs. Mg), and high ionic conductivity ( $8.5 \text{ mS cm}^{-1}$ ). Magnesium/sulfur cells employing the as-prepared electrolyte exhibited good cycling performance over 20 cycles in the range of 0.3–2.6 V, thus indicating an electrochemically reversible conversion of S to MgS without severe passivation of the Mg metal electrode surface.

The ever-increasing demands for energy and depleting fossil-fuel resources have made the development of renewable energy sources and advanced energy-storage technologies a global imperative.<sup>[1]</sup> Among all developed energy-storage devices, rechargeable lithium-ion batteries represent the state-of-the-art technology that are widely used in portable electronics. However, the inadequate rate of improvement in energy density and cycle life, as well as cost and safety concerns, means that it is difficult for lithium-ion batteries to meet the rapidly growing demand of the emerging markets of electric vehicles and grid energy storage. Therefore, the development of new electrochemical storage systems using safe, green, and low-cost electrode materials with high theoretical capacities is urgently needed.

Sulfur has recently received intensive research interest because of its advantages of inexpensiveness, abundance, and nontoxicity, as well as its high theoretical specific capacity of  $1675 \text{ mA h g}^{-1}$  and high theoretical volumetric capacity of  $3459 \text{ mA h cm}^{-3}$ , making it one of the most promising cathode materials for the development of next-generation energy-

storage systems. When coupled with a lithium metal anode, lithium/sulfur (Li/S) batteries have attracted great attention because of their great potential to deliver two to three times the energy density of current lithium-ion batteries.<sup>[2]</sup> In recent years, most efforts have been devoted to improving the efficiency and stable cycle behavior of Li/S cells, including sulfur cathodes,<sup>[3]</sup> electrolytes,<sup>[4]</sup> and separators.<sup>[5]</sup> For example, we previously found that cetyltrimethylammonium bromide (CTAB) modified graphene oxide (GO)–S and N-doped graphene (NG)–S nanocomposite cathodes could significantly improve the average Coulombic efficiency to above 99% and the cycle life of the Li/S cells up to 2000 cycles.<sup>[6]</sup> It has also been reported recently that employing solvent-in-salt electrolytes<sup>[7]</sup> or modified separators<sup>[8]</sup> are also an effective strategy for stabilizing the sulfur cathodes, which leads to boosted electrochemical performances in the corresponding Li/S cells. In the near future, it is believed that the performance of Li/S cells will meet the level of practical use. However, potential severe safety issues caused by the active nature of lithium metal and lithium dendrite still is a formidable challenge.

Magnesium is a promising anode candidate for pairing with the sulfur cathode. Unlike the Li anode, Mg can be safely used as a metal anode because repetitive Mg plating proceeds without dendrite formation. Furthermore, Mg is chemically inert, abundant in the earth's crust, and has a high theoretical volumetric capacity of  $3832 \text{ mA h cm}^{-3}$  because of its bivalent nature, significantly higher than  $2062 \text{ mA h cm}^{-3}$  of lithium.<sup>[9]</sup> Despite these advantages, magnesium/sulfur batteries are still in a very early stage of research, and prototype devices have been rarely demonstrated and realized.<sup>[10]</sup> To date, a suitable electrolyte for Mg/S cells has yet to be reported.

Magnesium salts in the electrolyte is one of the most important factors that affects the performance of Mg batteries.<sup>[11]</sup> Since the first electrochemically active complex  $[\text{Mg}_2(\mu\text{-Cl})_3(\text{THF})_6]^{2+}$  for a magnesium/sulfur (Mg/S) battery electrolyte was reported by Muldoon and co-workers in 2011,<sup>[10a]</sup> the preparation of non-nucleophilic Mg electrolytes has rapidly become a hot research topic. A common strategy is to combine an Mg complex, which may contain non-nucleophilic bases, with an aluminum- or boron-containing Lewis acid. Different Mg complexes, such as magnesium bis(hexamethyldisilazide)  $[(\text{HMDS})_2\text{Mg}]$ ,<sup>[10c]</sup>  $\text{ROMgCl}$ ,<sup>[12]</sup>  $\text{RSMgCl}$ ,<sup>[13]</sup>  $\text{MgCl}_2$ ,<sup>[14]</sup> were used to develop non-nucleophilic Mg electrolytes. However, crystallographic studies suggest that, independent of the initial forms of the Mg complexes used thus far, the same cationic complex unit  $[\text{Mg}_2(\mu\text{-Cl})_3(\text{THF})_6]^{2+}$  was observed in almost all of the salts crystallized from the corresponding organohaloaluminate or organobo-

[\*] Dr. W. Li, S. Cheng, J. Wang, Z. Zheng, Dr. H. Lin, S. Nanda, Q. Ma, Y. Xu, Dr. F. Ye, Dr. M. Liu, L. Zhou, Prof. Y. Zhang  
i-Lab, Suzhou Institute of Nano-Tech and Nano-Bionics  
Chinese Academy of Science, Suzhou Industrial Park  
Suzhou, Jiangsu, 215123 (P.R. China)  
E-mail: ygzhang2012@sinano.ac.cn

Dr. Y. Qiu, Prof. Y. Zhang  
Department of Physics, Tsinghua University  
Beijing, 100084 (China)

Supporting information (including general experimental details and characterization data) and the ORCID identification number(s) for the author(s) of this article can be found under <http://dx.doi.org/10.1002/anie.201600256>. CCDC 1433360 contains the supplementary crystallographic data for this paper. These data can be obtained free of charge from The Cambridge Crystallographic Data Centre via [www.ccdc.cam.ac.uk/data\\_request/cif](http://www.ccdc.cam.ac.uk/data_request/cif).

rate electrolytes in tetrahydrofuran (THF) solution. Chlorides in such a cation  $[\text{Mg}_2(\mu\text{-Cl})_3(\text{THF})_6]^{2+}$  have been identified as a major cause of corrosion,<sup>[15]</sup> therefore developing non-chlorinated electrolytes in overcoming the corrosion issue is essential to magnesium electrolytes that contain the  $[\text{Mg}_2(\mu\text{-Cl})_3(\text{THF})_6]^{2+}$  cation. Furthermore, this cation complex consists of two octahedrally coordinated Mg atoms bridged by three chlorides and paired with a counteranion. Such a bulky binuclear cation is detrimental to the transport of magnesium ions in the electrolyte and at the electrolyte–electrode interface.

A large number of early studies suggested that simple salts (i.e., mononuclear metal cation salts) of Mg ( $\text{MgCl}_2$ ,  $\text{Mg}(\text{ClO}_4)_2$ , etc.) fail to work in Mg systems because they easily passivate the Mg metal surface and prevent further cycling.<sup>[9a,16]</sup> On the other hand, from the perspective of practical applications, searching for a simple, low-cost, and effective simple electrolyte system based on a magnesium salt is very meaningful for efficient rechargeable Mg batteries. Very recently, Mohtadi and co-workers prepared a simple salt  $\text{Mg}(\text{CB}_{11}\text{H}_{12})_2$  with monocarborane  $\text{CB}_{11}\text{H}_{12}^-$  as a counteranion through a complicated synthetic procedure;<sup>[17]</sup> this salt showed a good performance in rechargeable magnesium batteries. However, they did not apply the electrolyte to an Mg/S battery. To the best of our knowledge, a simple magnesium salt based electrolyte for Mg/S batteries has not been reported to date. Herein we demonstrate, for the first time, a feasible strategy to synthesize a simple chloride-free  $[\text{Mg}(\text{THF})_6]^{2+}$  cation salt with  $\text{AlCl}_4^-$  as a counteranion by a simple heating method in an ionic liquid solvent. The electrolyte composed of the  $[\text{Mg}(\text{THF})_6][\text{AlCl}_4]_2$  salt and ionic liquid/THF cosolvents showed excellent Mg deposition behavior, anodic stability, and ionic conductivity. Mg/S cells using the mononuclear Mg electrolyte showed good cycling performance. This work provides a new electrolyte with a more simple structure and better compatibility with Mg/S batteries than the previously reported  $[(\text{Mg}_2(\mu\text{-Cl})_3\cdot 6\text{THF})]^{2+}$  cation.

The synthetic route and crystal structure of the  $[\text{Mg}(\text{THF})_6][\text{AlCl}_4]_2$  salt are shown in Figure 1. We identified the advantages of ionic liquids such as high boiling point, low melting point, high chemical and thermal stability, non-flammability, and low vapor pressure,<sup>[18]</sup> and proposed a stoichiometric reaction of  $\text{MgCl}_2$  (1 molar equiv) with  $\text{AlCl}_3$  (2 molar equiv), employing the ionic liquid *n*-methyl-*n*-butyl pyrrolidinium bis(trifluoromethanesulfonyl)imide (PYR14TFSI) as a reaction solvent. It was anticipated that the chloride ions in  $\text{MgCl}_2$  could be completely removed by  $\text{AlCl}_3$  with increasing temperature.

As expected, electrochemically active species comprising the  $[\text{Mg}(\text{THF})_6]^{2+}$  complex as the cation and  $[\text{AlCl}_4]^-$  as the counteranion were synthesized by reacting  $\text{MgCl}_2$  with two equivalents of  $\text{AlCl}_3$  in the ionic liquid PYR14TFSI at 95 °C for 24 h (see experimental details in the Supporting Information). The ionic conductivity of 0.3 M  $[\text{Mg}(\text{THF})_6][\text{AlCl}_4]_2$ /PYR14TFSI/THF electrolyte was determined to be  $8.5 \text{ mS cm}^{-1}$  at room temperature (see the Supporting Information for details). This conductivity is much higher than the values of other Mg electrolytes.<sup>[12a,13,14]</sup>

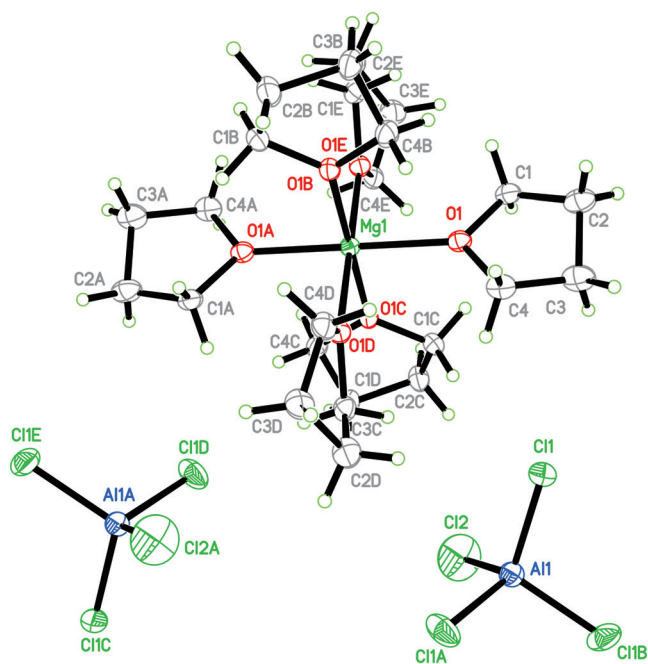
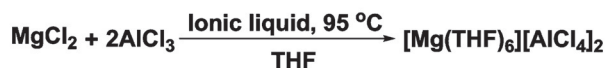


**Figure 1.** Proposed formation mechanism and X-ray crystal structure of Mg salt.

The molecular structure obtained was characterized by single-crystal X-ray diffraction, and crystals suitable for X-ray structure determination were grown and obtained from cold PYR14TFSI/THF solution (see the Supporting Information). The crystal structure of  $[\text{Mg}(\text{THF})_6][\text{AlCl}_4]_2$  showed that the chloride ions of  $\text{MgCl}_2$  were completely removed by  $\text{AlCl}_3$  to leave  $\text{Mg}^{2+}$  ions, which coordinated to the solvent molecules to form the single-nuclear cation  $[\text{Mg}(\text{THF})_6]^{2+}$  (see Table S1 in the Supporting Information for details of the intensity data collection and crystal data). The presence of the  $\text{AlCl}_4^-$  ion was further proved from its characteristic peak at about  $350 \text{ cm}^{-1}$  in the Raman spectrum (Figure S1).<sup>[19]</sup>

To identify the Mg electrochemical deposition behavior with the  $[\text{Mg}(\text{THF})_6]^{2+}$  cation electrolyte, cyclic voltammetry (CV) measurements with a Pt disk as the working electrode and Mg foil as both reference and counterelectrodes were examined at a scan rate of  $25 \text{ mV s}^{-1}$  in the potential range of  $-1$  to  $2 \text{ V}$  (vs.  $\text{Mg}/\text{Mg}^{2+}$ ). As shown in Figure 2a, the reduction peak at about  $-0.6 \text{ V}$  corresponds to the deposition of Mg metal. In the subsequent oxidation step, the onset for the oxidation voltage was seen at about  $0.2 \text{ V}$ , determined by the turning point at which a rapid increase in the current density was clearly observed. The oxidation peak with maximum current density at about  $0.5 \text{ V}$  is attributed to the subsequent electrochemical dissolution of the Mg metal. The peaks are then shifted to  $-0.5 \text{ V}$  and  $0.5 \text{ V}$  respectively in the following cycles, and the height and position of the oxidation peak both remain relatively stable with repeated cycling, thus indicating a more stable reversibility of Mg deposition and dissolution. When Cu foil was selected as the working

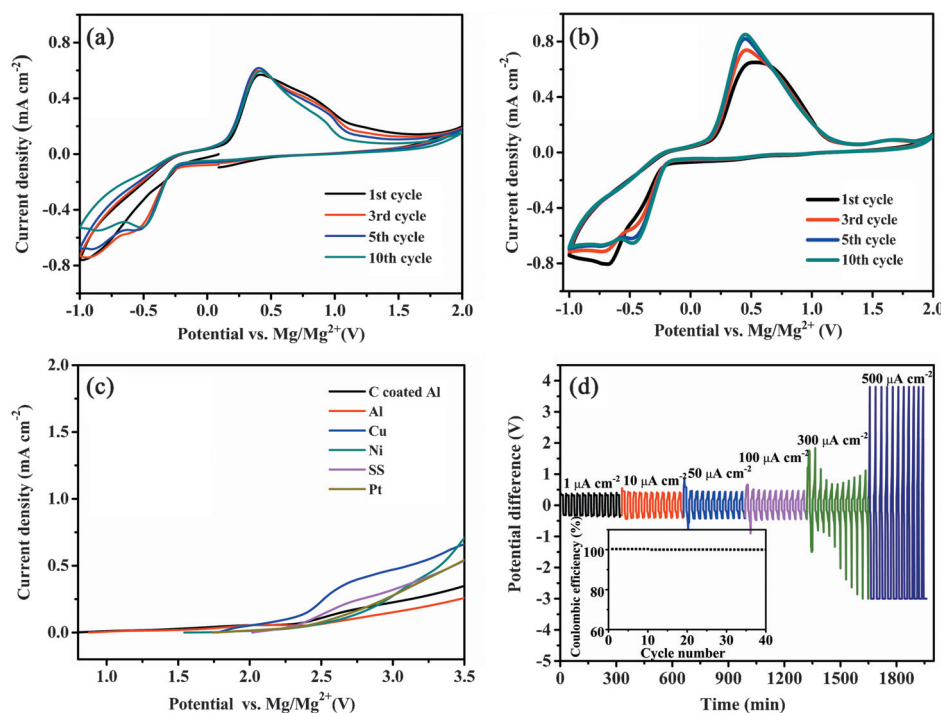


**Figure 2.** Cyclic voltammogram of electrolyte  $[\text{Mg}(\text{THF})_6][\text{AlCl}_4]_2$  in PYR14TFSI/THF (1:1 v/v). The working electrodes are a) Pt disk and b) Cu foil while the counter- and reference electrodes are Mg metal. Measurements obtained at  $25 \text{ mV s}^{-1}$  and under ambient conditions. c) The LSV of electrolyte  $[\text{Mg}(\text{THF})_6][\text{AlCl}_4]_2$  in PYR14TFSI/THF (1:1 v/v) on different working electrodes while the counter- and reference electrodes are Mg metal. Measurements obtained at  $25 \text{ mV s}^{-1}$  and ambient conditions. d) Cycling behavior of a symmetrical cell with electrolyte  $[\text{Mg}(\text{THF})_6][\text{AlCl}_4]_2$  in PYR14TFSI/THF (1:1 v/v) at different current densities of  $1 \mu\text{A cm}^{-2}$  to  $500 \mu\text{A cm}^{-2}$ . The cycle time was 30 min per cycle (15 min charging and 15 min discharging).

electrode, similar results were observed, as shown as Figure 2b. It is clearly evident from the cyclic voltammograms that the process of magnesium deposition and dissolution in the as-synthesized electrolyte is highly reversible.

The electrochemical oxidative stabilities of the  $[\text{Mg}(\text{THF})_6][\text{AlCl}_4]_2/\text{PYR14TFSI}:\text{THF}$  electrolyte were further investigated by linear sweep voltammetry using different electrode materials. As illustrated in Figure 2c, all electrodes display a similar oxidation onset potential in a narrow range between 2.5–3.0 V. Although the anodic stability is not better than the reported chloride-free Mg organoborate electrolytes,<sup>[17]</sup> our simple Mg salt electrolyte with a chloride-free cation showed an oxidative stability which is comparable to that of that formed in situ (ca. 2.5 V) but lower than that of the crystal-based (3.2 V) Mg organohaloaluminate electrolyte  $([\text{Mg}_2(\mu\text{-Cl})_3(\text{THF})_6][\text{HMDS}_n\text{AlCl}_{4-n}]_2 (n = 1 \text{ or } 2))$ .<sup>[10a,15]</sup> Compared to the Mg organoborate salts with high anodic stabilities, the new Mg salt was fabricated directly from commercial available starting materials by using a simple, highly scalable, and low-cost approach.

Symmetric  $\text{Mg} | 0.3 \text{ M } [\text{Mg}(\text{THF})_6][\text{AlCl}_4]_2/\text{PYR14TFSI}:\text{THF} | \text{Mg}$  cells were assembled for evaluating electrolyte performance. The magnesium stripping/plating experiment was first conducted by cycling over 15 minute charging and discharging intervals under different current densities from  $1 \mu\text{A cm}^{-2}$  to  $500 \mu\text{A cm}^{-2}$ . As shown in Figure 2d and its

inset, the cell showed an excellent Coulombic efficiency close to 100% at low current density, but experienced a higher degree of polarization and irregular potential variation when the current density increased to  $300 \mu\text{A cm}^{-2}$ . Figure 3a shows that the cell could be cycled 100 times without a significant increase in polarization at a current density of  $50 \mu\text{A cm}^{-2}$ . This behavior suggests that there is only a very minor reaction occurring between the magnesium electrode and the mononuclear Mg electrolyte system at low current densities.

To further investigate the formation and stability of the interface between the electrolyte solution and the magnesium electrode during cycling, electrochemical impedance spectroscopy (EIS) measurements were performed. As shown in Figure 3b, the bulk resistance of the electrolyte is the intercept on the x-axis at a high frequency, which is very low and almost constant with increasing cycle number (inset of Figure 3b). While the high frequency semi-

circle corresponds to the interfacial resistance, which remarkably decreased over 80 cycles and then no obvious change was observed for the following cycles. This behavior indicates that the interface between the magnesium electrode and the electrolyte solution was unstable during the initial cycling stage, and the solid electrolyte interface (SEI) layer of the magnesium electrode can stabilize after a certain number of cycles.

As a new member of the magnesium organohaloaluminate family, the simple Mg salt of  $[\text{Mg}(\text{THF})_6][\text{AlCl}_4]_2$  used in this work does not contain chloride species in the cation. The excellent efficiency and stability from this study of the electrolyte properties encouraged us to demonstrate its potential for use in a reversible Mg/S battery. As shown in Figure 4a, the NG-S cathode delivers an initial discharge capacity of  $700 \text{ mA h g}^{-1}$  (based on the mass of sulfur,  $1 \text{ C} = 1675 \text{ mA h g}^{-1}$ ) and a potential plateau of 0.8 V at rate of 0.01 C for discharging and 0.02 C for charging, which is similar to the Mg/C-S cell with 0.4 M  $[\text{Mg}_2(\mu\text{-Cl})_3(\text{THF})_6][\text{HMDSA}(\text{AlCl}_3)]$  in THF (potential plateau of 0.89 V),<sup>[10a]</sup> and higher than that of Mg/CMK3-S cell with 0.3 M  $\text{Mg}(\text{TFSI})_2$  in glyme/diglyme (potential plateau of 0.2 V),<sup>[10b]</sup> most likely arising from the improvement of surface layer on the magnesium anode in the presence of our electrolyte. The overcharging behavior observed in Figure 4a is consistent with previous reports and is due to polysulfide dissolution in



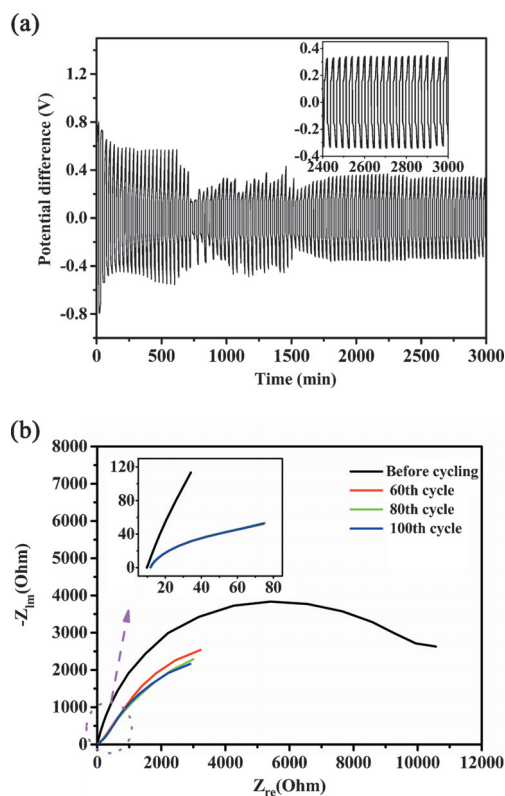


**Figure 3.** a) Cycling behavior of a symmetrical cell with electrolyte  $[\text{Mg}(\text{THF})_6][\text{AlCl}_4]_2$  in PYR14TFSI/THF (1:1 v/v) at a current density of  $50 \mu\text{A cm}^{-2}$ . The cycle time was 30 min per cycle (15 min charging and 15 min discharging). b) EIS for different cycling times of a Mg/Mg symmetrical cell with electrolyte  $[\text{Mg}(\text{THF})_6][\text{AlCl}_4]_2$  in PYR14TFSI/THF (1:1 v/v) at a current density of  $50 \mu\text{A cm}^{-2}$ . The cycle time was 30 min per cycle (15 min charging and 15 min discharging).

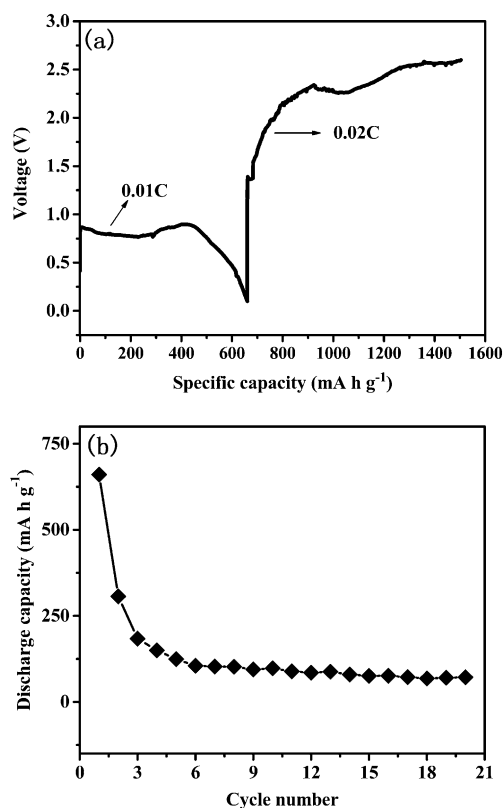


**Figure 4.** Discharge and charge profile for a) first cycle and b) 20 cycles of discharging and charging. Cathode: 50% S loading, NG/SP/Commercial S/PVDF = 4:5:10:1 Rate: 0.01 C discharging, 0.02 C charging. Anode: Mg disk.

the electrolyte. The Mg/S cell cycling performance is shown in Figure 4b. The cell can cycle stably for more than 20 cycles, with its capacity rapidly decreased from about  $700 \text{ mA h g}^{-1}$  to  $130 \text{ mA h g}^{-1}$  in the first 5 cycles, after which a comparatively stabilized capacity of  $70 \text{ mA h g}^{-1}$  was observed. These cycle performances were considerably improved compared to previous work on Mg/S batteries where an Mg salt of  $[\text{Mg}_2(\mu\text{-Cl})_3(\text{THF})_6][\text{HMDSAICl}_3]$  was used as solute in THF, and are very close to that in very recently study employing a electrolyte of  $[\text{Mg}_2\text{Cl}_3][\text{HMDSAICl}_3]$  in binary solvents of glyme and ionic liquid.<sup>[10c]</sup>

To understand the reason for the reduction in capacity, we explored the morphology and structural change of the NG-S electrode and the interface between the electrolyte and Mg anode after repeated Mg insertion/extraction. The cell that was electrochemically evaluated at 0.01 C for discharging and 0.02 C for charging for 20 cycles was disassembled and characterized by using SEM. The results are displayed in Figure 5. Before cycling, the NG-S cathode surface shows the typical electrode morphology, namely rough without any cracks. After 20 cycles, the NG-S electrode became dense and obvious cracks were observed, which would lead to poor electric conductivity and reduction in capacity. Compared to the smooth surface of original Mg, it was found that the Mg

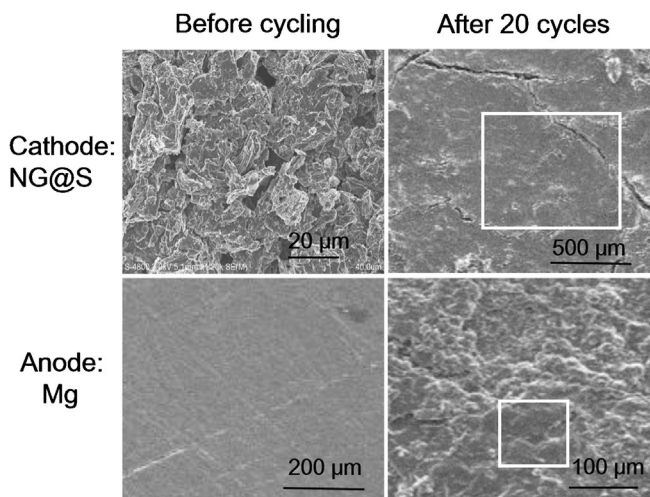


**Figure 5.** Morphologies of S cathode and Mg anode before and after 20 cycles of charging and discharging.

surface became rough and an evident film on the Mg electrode was formed with no Mg dendrites on the Mg electrode observed after 20 cycles. Elemental compositions of NG@S electrode and Mg anode analyzed by energy-dispersive X-ray (EDX) microanalysis are shown in Table S2. The corresponding EDX results showed evidence of a sulfur

component on the anode surface, and the loss of sulfur on the cathode suggest the existence of a shuttle mechanism in the Mg/S battery. While we did not observe any sulfur species on the Mg anode of a Mg/Mg symmetrical cell with the  $[\text{Mg}(\text{THF})_6][\text{AlCl}_4]_2$  electrolyte in PYR14TFSI/THF (1:1 v/v) after 100 cycles of charging and discharging at a current density of  $50 \mu\text{A cm}^{-2}$ . Hence, the capacity fading of the batteries was most likely caused by the shuttling of polysulfides from the cathode.

In summary, a simple  $[\text{Mg}(\text{THF})_6]^{2+}$  cation salt with  $\text{AlCl}_4^-$  counteranions was synthesized by a facile heating method in ionic liquid solvent, and structurally characterized by X-ray diffraction analysis. The utility of an ionic liquid as a reaction solvent to completely remove the chloride ions from  $\text{MgCl}_2$  by the Lewis acid  $\text{AlCl}_3$  has been reported for the first time. An Mg electrolyte based on the as-prepared complex of  $[\text{Mg}(\text{THF})_6][\text{AlCl}_4]_2$  possesses a highly reversible Mg cycling behavior ( $>100$  cycles), good anodic stability (2.5 V vs. Mg), and good ionic conductivity ( $8.5 \text{ mS cm}^{-1}$ ). The new electrolyte proved to be efficient for a magnesium battery with a sulfur cathode. The present strategy has potential in the development of rechargeable Mg/S battery electrolytes.

## Acknowledgements

We thank Dr. J. H. Liu, and Prof. X. W. Yang for helpful discussions. We acknowledge support from the National Natural Science Foundation of China (No. 21433013) and Suzhou Science and Technology Development Program (No. ZXG2013002, SYG201532).

**Keywords:** electrochemistry · electrolytes · magnesium · rechargeable batteries · sulfur

**How to cite:** *Angew. Chem. Int. Ed.* **2016**, *55*, 6406–6410  
*Angew. Chem.* **2016**, *128*, 6516–6520

- [1] D. Larcher, J. M. Tarascon, *Nat. Chem.* **2015**, *7*, 19–29.
- [2] Y. X. Yin, S. Xin, Y. G. Guo, L. J. Wan, *Angew. Chem. Int. Ed.* **2013**, *52*, 13186–13200; *Angew. Chem.* **2013**, *125*, 13426–13441.
- [3] a) Y. Yang, G. Zheng, Y. Cui, *Chem. Soc. Rev.* **2013**, *42*, 3018; b) M. A. Pope, I. A. Aksay, *Adv. Energy Mater.* **2015**, *5*, 1500124.
- [4] S. Zhang, K. Ueno, K. Dokko, M. Watanabe, *Adv. Energy Mater.* **2015**, *5*, 1500117.
- [5] J.-Q. Huang, Q. Zhang, F. Wei, *Energy Storage Mater.* **2015**, *1*, 127–145.
- [6] a) Y. Qiu, W. Li, W. Zhao, G. Li, Y. Hou, M. Liu, L. Zhou, F. Ye, H. Li, Z. Wei, S. Yang, W. Duan, Y. Ye, J. Guo, Y. Zhang, *Nano Lett.* **2014**, *14*, 4821–4827; b) M. K. Song, Y. Zhang, E. J. Cairns, *Nano Lett.* **2013**, *13*, 5891–5899.
- [7] L. Suo, Y. S. Hu, H. Li, M. Armand, L. Chen, *Nat. Commun.* **2013**, *4*, 1481.
- [8] a) J. Q. Huang, T. Z. Zhuang, Q. Zhang, H. J. Peng, C. M. Chen, F. Wei, *ACS Nano* **2015**, *9*, 3002–3011; b) G. Zhou, L. Li, D. W. Wang, X. Y. Shan, S. Pei, F. Li, H. M. Cheng, *Adv. Mater.* **2015**, *27*, 641–647; c) S.-H. Chung, A. Manthiram, *J. Phys. Chem. Lett.* **2014**, *5*, 1978–1983.
- [9] a) D. Aurbach, I. Weissman, Y. Gofer, E. Levi, *J. Electrochem. Soc.* **1990**, *3*, 61–73; b) D. Aurbach, Z. Lu, A. Schechter, Y. Gofer, H. Gizbar, R. Turgeman, Y. Cohen, M. Moshkovich, E. Levi, *Nature* **2000**, *407*, 724–727; c) H. D. Yoo, I. Shterenberg, Y. Gofer, G. Gershtinsky, N. Pour, D. Aurbach, *Energy Environ. Sci.* **2013**, *6*, 2265.
- [10] a) H. S. Kim, T. S. Arthur, G. D. Allred, J. Zajicek, J. G. Newman, A. E. Rodnyansky, A. G. Oliver, W. C. Boggess, J. Muldoon, *Nat. Commun.* **2011**, *2*, 427; b) S. Y. Ha, Y. W. Lee, S. W. Woo, B. Koo, J. S. Kim, J. Cho, K. T. Lee, N. S. Choi, *ACS Appl. Mater. Interfaces* **2014**, *6*, 4063–4073; c) Z. Zhao-Karger, X. Zhao, D. Wang, T. Diemant, R. J. Behm, M. Fichtner, *Adv. Energy Mater.* **2015**, *5*, 1401155; d) T. Gao, M. Noked, A. J. Pearce, E. Gillette, X. Fan, Y. Zhu, C. Luo, L. Suo, M. A. Schroeder, K. Xu, S. B. Lee, G. W. Rubloff, C. Wang, *J. Am. Chem. Soc.* **2015**, *137*, 12388–12393.
- [11] a) J. Muldoon, C. B. Bucur, A. G. Oliver, T. Sugimoto, M. Matsui, H. S. Kim, G. D. Allred, J. Zajicek, Y. Kotani, *Energy Environ. Sci.* **2012**, *5*, 5941; b) P. Saha, M. K. Datta, O. I. Velikokhatnyi, A. Manivannan, D. Alman, P. N. Kumta, *Prog. Mater. Sci.* **2014**, *66*, 1–86; c) J. Muldoon, C. B. Bucur, T. Gregory, *Chem. Rev.* **2014**, *114*, 11683–11720.
- [12] a) R. E. Doe, R. Han, J. Hwang, A. J. Gmitter, I. Shterenberg, H. D. Yoo, N. Pour, D. Aurbach, *Chem. Commun.* **2014**, *50*, 243–245; b) C. Liao, B. Guo, D.-e. Jiang, R. Custelcean, S. M. Mahurin, X.-G. Sun, S. Dai, *J. Mater. Chem. A* **2014**, *2*, 581–584.
- [13] P. Bian, Y. NuLi, Z. Abudoureyimu, J. Yang, J. Wang, *Electrochim. Acta* **2014**, *121*, 258–263.
- [14] a) T. Liu, Y. Shao, G. Li, M. Gu, J. Hu, S. Xu, Z. Nie, X. Chen, C. Wang, J. Liu, *J. Mater. Chem. A* **2014**, *2*, 3430; b) B. Pan, J. Zhang, J. Huang, J. T. Vaughey, L. Zhang, S. D. Han, A. K. Burrell, Z. Zhang, C. Liao, *Chem. Commun.* **2015**, *51*, 6214–6217; c) Y. Cheng, R. M. Stolley, K. S. Han, Y. Shao, B. W. Arey, N. M. Washton, K. T. Mueller, M. L. Helm, V. L. Sprenkle, J. Liu, G. Li, *Phys. Chem. Chem. Phys.* **2015**, *17*, 13307–13314.
- [15] J. Muldoon, C. B. Bucur, A. G. Oliver, J. Zajicek, G. D. Allred, W. C. Boggess, *Energy Environ. Sci.* **2013**, *6*, 482–487.
- [16] Z. Lu, A. Schechter, M. Moshkovich, D. Aurbach, *J. Electroanal. Chem.* **1999**, *466*, 203–217.
- [17] O. Tutasaus, R. Mohtadi, T. S. Arthur, F. Mizuno, E. G. Nelson, Y. V. Sevryugina, *Angew. Chem. Int. Ed.* **2015**, *54*, 7900–7904; *Angew. Chem.* **2015**, *127*, 8011–8015.
- [18] C. Ruß, B. König, *Green Chem.* **2012**, *14*, 2969.
- [19] M. C. Lin, M. Gong, B. Lu, Y. Wu, D. Y. Wang, M. Guan, M. Angell, C. Chen, J. Yang, B. J. Hwang, H. Dai, *Nature* **2015**, *520*, 324–328.

Received: January 11, 2016

Published online: April 20, 2016